Yoderite, a new hydrous magnesium iron alumino-silicate from Mautia Hill, Tanganyika.

(With Plate XI.)

By DUNCAN MCKIE, M.A., B.Sc., A.R.I.C., F.G.S.
Dept. of Mineralogy and Petrology, Downing Place, Cambridge.

With chemical analyses by A. J. RADFORD, B.Sc., F.R.I.C.
Geological Survey, Causeway, Salisbury, Southern Rhodesia.

[Read 6 November 1958.]

Summary. Yoderite occurs as a major constituent in a quartz–kyanite–talc schist, and is a high-pressure phase formed by the reaction Ky + Tc → Yd + Qu. The monoclinic unit-cell, a 8·10 Å., b 5·78 Å., c 7·28 Å., β 106°, space-group $P2_1$ or $P2_1/m$, contains approximately $(Mg_{2\cdot0}Ca_{0\cdot2}Fe_{0\cdot5}Al_{5\cdot3})Si_{4\cdot0}O_{17\cdot6}(OH)_{2\cdot4}$. The structure appears to be related to that of kyanite, with which the mineral is intergrown; it is not an analogue of staurolite. The three strongest powder lines are 3·50 Å. vvs, 3·03 Å. vs, 2·61 Å. s. Specific gravity 3·39. Subsidiary reflections, similar to those of the intermediate plagioclases, have indices with non-simple fractional values of k. Optical properties are α 1·689 pale Prussian blue, β 1·691 indigo, γ 1·715 light olive-green, absorption $\beta > \alpha > \gamma$, $2V_\gamma$ 25°, optic axial plane {010}, γ:[001] $\approx$ 7° in the obtuse angle β. An interpretation of the colour on the electron-exchange hypothesis $Fe^{2+} \rightleftharpoons Fe^{3+} + e^-$, is suggested. A kinetic study has been made of the disappearance of the subsidiary reflections in the range 700° C. to 820° C.; further heating to 850° C. produces the metastable appearance of mullite, and at temperatures above 1100° C. the equilibrium anhydrous assemblage indialite + sapphirine appears.

YODERITE, a spectacular purple mineral, occurs in a quartz–yoderite–kyanite–talc schist at Mautia Hill (6° 8½′ S., 36° 29′ E.), 6 miles north-east of the former Groundnut Scheme headquarters at Kongwa, Mpwapwa District, Central Province, Tanganyika Territory. The general geology of the district has been described by Temperley (1938), who regarded (p. 40) the yoderite-bearing rocks as glaucophane–kyanite–magnetite–muscovite–quartz schists and observed that 'glaucophane' always surrounds kyanite; a more detailed account of the petrology of Mautia Hill is in course of preparation by the author and J. R. Harpum. Mautia Hill is an east–west ridge, 2 miles long by ½ mile wide, of metamorphic rocks of the Usagaran System (Archaean), consisting of steeply dipping units of east–west striking crystalline lime-

stone, quartzite, piemontite–quartzite, kyanite–biotite gneiss, quartz–yoderite–kyanite–talc schist, and amphibolite, the whole completely surrounded by the poorly exposed migmatites of the Kongwa plains. No recognizable continuation of the distinctive Mautia succession appears to occur either to the east or the west.

The mineral is named in honour of Dr. H. S. Yoder, Jr., of the Geophysical Laboratory, Carnegie Institution of Washington, who first studied experimentally the central part of the MgO–Al_2O_3–SiO_2–H_2O system, within which 92 % of the composition of yoderite lies.

Yoderite has in the past been mistaken for glaucophane and for dumortierite, the characteristic pleochroism of which is closely similar; it was first recognized as a distinct mineral by its X-ray powder pattern.

Petrography. The quartz–yoderite–kyanite–talc schist is composed of coarse interlocking, often curved, flakes of talc with interstitial patches of quartz, exhibiting strain shadows; large irregularly margined grains of yoderite enclose random flakes of talc and some quartz. The general aspect of the rock is shown in pl. XI, fig. 1. A constant feature is the presence within each yoderite grain of relicts of kyanite (pl. XI, fig. 3), and kyanite occurs rimmed by yoderite (pl. XI, fig. 4). Quartz and talc occur on the outer margins of yoderite grains; the replacement of talc by yoderite is shown in pl. XI, fig. 2. Small rounded grains of hematite are randomly distributed through all other minerals. Yoderite and kyanite both contain large rounded quartz inclusions (pl. XI, figs. 3, 4); less regular patches of quartz also occur within yoderite grains. Every yoderite grain, however large and poikiloblastic, is optically a single crystal and all the kyanite relicts within it are in parallel orientation. Yoderite invariably separates talc from kyanite; assemblages present are quartz–yoderite–kyanite–hematite and quartz–yoderite–talc–hematite.

The proportions of quartz and talc vary markedly from the common talc-rich schistose type to a talc–yoderite–kyanite–quartzite. Yoderite has been studied from two specimens, a talc-rich type bearing the Geological Survey of Tanganyika number JH 2563/2 and a quartz-rich type numbered JH 2563/14.

Chemical composition.

Yoderite from specimen JH 2563/2 was freed from talc and quartz by centrifugal separation of −60 mesh +120 mesh material in methylene iodide, followed by electromagnetic removal of hematite, repeated electromagnetic separation of weakly magnetic yoderite from kyanite,

and finally hand-picking. Some 2 g. were available for the main analysis and a further portion, crushed to −90 mesh +120 mesh, was very carefully picked free of hematite-contaminated grains for the iron determinations.

The analysis is set down in table I and corresponds to the formula $(Mg_{2\cdot0}Ca_{0\cdot2}Fe_{0\cdot5}Al_{5\cdot3})Si_{4\cdot0}O_{17\cdot6}(OH)_{2\cdot4}$. H_2O+ was determined by direct weighing of the water evolved on ignition at 1100° C. in a tube furnace. The marked insolubility of yoderite made the determination of FeO

TABLE I. Chemical composition and unit-cell contents of yoderite.

		1.	2.			3.	4.	
SiO_2	...	36·12	36·07	Si^{4+}	...	0·6006	4·00	4·03
TiO_2	...	0·35	0·35	Ti^{4+}	...	0·0044	0·03	
Al_2O_3	...	41·06	41·00	Al^{3+}	...	0·8041	5·35	8·06
Fe_2O_3	...	0·50	0·50	Fe^{3+}	...	0·0063	0·04	
FeO	...	4·82	4·81	Fe^{2+}	...	0·0670	0·45	
MnO	...	0·32	0·32	Mn^{2+}	...	0·0045	0·03	
MgO	...	12·23	12·21	Mg^{2+}	...	0·3028	2·02	
CaO	...	1·48	1·48	Ca^{2+}	...	0·0262	0·17	
Na_2O	...	0·01	0·01	Na^{+}	...	0·0003	—	
K_2O	...	0·05	0·05	K^{+}	...	0·0011	—	
H_2O+	...	3·20	3·20	OH^{-}	...	0·3552	2·36	20·00
H_2O-	...	0·05	—	O^{2-}	...	2·6495	17·64	
		100·19	100·00					

1. Analysis of yoderite from specimen JH 2563/2. Analyst: A. J. Radford.
2. Analysis 1 recalculated to 100 % on an H_2O- free basis.
3. Atomic ratios.
4. Unit-cell contents corresponding to 20 anions per unit cell.

difficult; the method of Groves (1951, p. 183) proved unsatisfactory and I am indebted to Mr. J. H. Scoon[1] for a redetermination using Hey's (1941) micro-method, the result of which is quoted in table I. Cu, Pb, Co, Ni, B, and P were sought and found not to be present in significant amounts. Dr. S. R. Nockolds[1] confirmed the absence of Cu, Co, F, and B spectrographically.

Physical properties.

Yoderite occurs in anhedral, irregularly lath-shaped grains up to $\frac{1}{2}\times\frac{1}{4}\times\frac{1}{8}$ inches. Its hardness is 6 on Mohs' scale. Measurements of specific gravity by displacement of methylene iodide from a specific gravity bottle gave a value of 3·39. Refractive indices at 20° C. are α 1·689, β 1·691, γ 1·715 (all ±0·002); and $2V_\gamma$ 25° (±2°). The pleochroic

[1] Department of Mineralogy and Petrology, University of Cambridge.

scheme is α pale Prussian blue, β indigo, γ light olive-green, with absorption $\beta > \alpha > \gamma$. In the absence of crystal faces and good cleavages the orientation of the optical indicatrix had to be determined by direct reference to the chosen monoclinic crystallographic axes; optical direc-

TABLE II. X-ray powder data for yoderite.

d, Å.	*I.*	*d*, Å.	*I.*	*d*, Å.	*I.*	*d*, Å.	*I.*
4·64	w	1·97	m	1·219	vw	0·909	vvw
4·18	vvw	1·89	w	1·210	vw	0·893	vvw
3·87	vw	1·84	vvw	1·202	vw	0·891	vvw
3·83	vw	1·82	s	1·197	vw	0·888	vvw
3·63	w	1·752	vvw	1·175	vvw	0·883	vvw
3·50	vvs	1·727	m	1·166	vvw	0·863	vvw
3·34	vvw	1·698	vw	1·101	vvw	0·861	vvw
3·23	ms	1·647	vw	1·076	vwB	0·845	vvw
3·19	ms	1·610	w	1·058	vvw	0·843	vvw
3·07	vw	1·596	w	1·054	vvw	0·8375	vvw
3·03	vs	1·561	vvw	1·041	vvw	0·8360	vvw
2·91	ms	1·547	w	1·038	vvw	0·8306	vvw
2·72	vw	1·534	w	1·033	vw	0·8284	vvw
2·68	m	1·515	w	1·007	vw	0·8256	vvw
2·65	vw	1·499	wB	1·005	vvw	0·8232	vw
2·61	s	1·473	wB	0·999	w	0·8184	vvw
2·58	ms	1·451	m	0·997	vw	0·8165	vvw
2·46	ms	1·437	vw	0·985	vw	0·8142	vvw
2·41	vvw	1·415	w	0·983	vvw	0·8131	vvw
2·39	mw	1·399	mw	0·977	vvw	0·8110	vvw
2·36	w	1·382	vwB	0·973	vvw	0·8085	vvw
2·32	w	1·356	m	0·967	vw	0·8051	vvw
2·27	vw	1·340	vw	0·964	vvw	0·8029	vvw
2·24	msB	1·328	m	0·945	vw	0·8005	vvw
2·16	vw	1·298	vw	0·943	vvw	0·7979	vvw
2·11	vw	1·286	vvw	0·939	vw	0·7957	vvw
2·06	vvw	1·265	vvw	0·925	vvw	0·7865	vvw
2·00	s	1·240	vvw	0·915	vvw	0·7785	vvw

X-ray powder data for the analysed sample of yoderite (JH 2563/2). Relative intensities *I* were estimated visually. A camera of 19 cm. diameter and Cu-$K\alpha$ radiation were used.

tions in a grain were labelled by attaching glass fibres and the grain was then completely oriented by a zero-layer *b*-axis Weissenberg photograph. The optic axial plane is {010}, $\alpha \wedge a \approx 9°$ and $\gamma \wedge c \approx 7°$, both in the obtuse β-angle. Parting directions are [001] moderately good and {100} poor. Grains are elongated parallel to [010] and longitudinal sections can therefore be length fast or length slow.

X-ray powder data for yoderite are presented in table II; 112 lines were measured. The three strongest lines are: 3·50 Å. vvs, 3·03 Å. vs,

2·61 Å. s. The iron content of the mineral is not high enough to produce any serious fluorescent fogging with Cu-$K\alpha$ radiation.

X-ray crystallography.

In the single-crystal study of yoderite grains were used from specimens JH 2563/2 and JH 2563/14; no differences were observed in the diffraction patterns. The symmetry of a *b*-axis oscillation photograph and that of a zero-layer Weissenberg photograph about the *b*-axis show that the mineral is monoclinic. The unit-cell dimensions and space-group were determined from oscillation photographs about the *a*, *b*, and *c* axes, and from zero and fourth layer Weissenberg photographs about the *a*-axis. The unit-cell dimensions are *a* 8·10 Å., *b* 5·78 Å., *c* 7·28 Å. (all $\pm$0·05 Å.), and β 106° ($\pm$1°); $a:b:c = 1{\cdot}402:1:1{\cdot}259$. The only systematic absences were $0k0$ with k odd. Certain extra weak reflections that cannot be indexed on the lattice described above were observed on all over-exposed photographs and will be discussed below. The space-group of the pseudo-lattice is therefore $P2_1$ or $P2_1/m$; a positive pyroelectric effect suggests that $P2_1$ is the more likely.

The unit-cell volume 328 Å.^{3} corresponds to the unit-cell contents shown in column 4 of table I, or to $\{X_2Si(O,OH)_5\}$, analogous to the aluminium silicate formula Al_2SiO_5 with some replacement of Al and O, all positions being occupied and no Si replaced. Al^{3+} is replaced essentially by Mg^{2+}, Fe^{2+}, Fe^{3+}, and Ca^{2+}, one-third of the Al^{3+} ions being replaced; the charge deficiency is compensated by the substitution of 2·35 OH^- for O^{2-}. The volume per oxygen atom is 16·4 Å.^{3}, compared with 14·2 Å.^{3} in kyanite (where the oxygen ions are approximately in cubic close packing), 16·2 Å.^{3} in sillimanite, 15·2 Å.^{3} in staurolite, and 17·1 Å.^{3} in mullite increasing to 17·5 Å.^{3} in synthetic iron-rich mullites.

Yoderite is seen in thin-section to contain relicts of kyanite in constant optical orientation. An oscillation photograph of a composite grain about the *b*-axis of yoderite indicated *b* (yoderite) || *c* (kyanite), and a zero layer Weissenberg photograph about this common axis gave a complete account of the relative orientation, which is shown in fig. 1. Extra reflections on the Weissenberg photograph show that kyanite in this grain is twinned about the normal to {100}, a not uncommon twin law in kyanite. *b* 5·78 Å. of yoderite is similar and parallel to *c* 5·56 Å. of kyanite, representing the length of two octahedral groups in the aluminium-oxygen chains, a common feature of the unit cells of all the aluminium silicates; *a* 8·10 Å. for yoderite is similar and parallel to *b* 7·72 Å. for kyanite; *c* 7·28 Å. for yoderite is not dissimilar to *a* sin β

6·96 Å. for kyanite. Thus the yoderite unit cell is expanded by about 5 % in the a and c directions relative to kyanite, and by 4 % in the direction of the aluminium-oxygen chains, b_Y being similar to the corresponding parameter a 5·74 Å. of sillimanite. Considerable structural similarity may thus be expected between yoderite and kyanite; chains of aluminium coordinated octahedrally to oxygen may be expected to

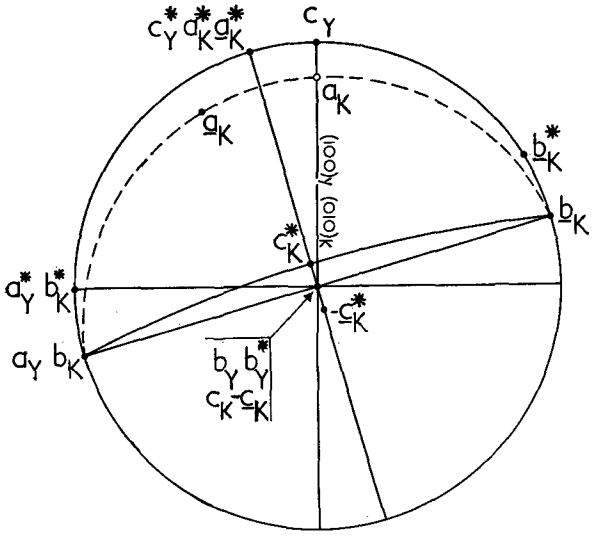

FIG. 1. Stereogram showing the relative orientation of yoderite (Y) and kyanite (K). Underlined symbols refer to the second individual of the kyanite twin.

run parallel to b, the chains being linked laterally by silicon in fourfold coordination and by aluminium probably in sixfold coordination as in kyanite. Aluminium, exhibiting sixfold coordination in both positions, may be designated Al_I in the chains and Al_{II} in the cross-linkages; the cations substituting for Al in yoderite all normally exhibit sixfold coordination and might therefore appear to replace Al in either position. The distribution of the 2·4 OH^- ions per unit cell may be random, but if the explanation of the colour of yoderite given below is correct and Weyl's (1951) interpretation of the pleochroic scheme of biotite is of general application the OH^- ions should be concentrated on planes perpendicular to the direction of minimum absorption γ, that is near $(\bar{1}06)$, which is parallel to $(6\bar{1}0)$ of kyanite, a plane, however, of no special significance in the kyanite structure.

Consideration of the atomic coordinates in kyanite (Naray-Szabo, Taylor, and Jackson, 1929) clarifies the structural relationship between yoderite and kyanite. Small displacements in the positions of atoms in the kyanite structure can give rise to a monoclinic $P2_1$ lattice, the largest adjustments being in the z-coordinates of Al in cross-linkages, Al_{III} and Al_{IV} of Naray-Szabo *et al.* The dimensions of the resultant unit-cell would be a' 6·96 Å., b' 7·72 Å., c 5·56 Å., β' 106°; it would be oriented with respect to the triclinic kyanite lattice in precisely the same way as yoderite was observed to be oriented in yoderite-kyanite intergrowths. The partial substitution of Mg^{2+} for Al^{3+} would appear to produce the requisite distortion, accompanied by an overall linear expansion of 4–5 %.

The orientation of staurolite with respect to kyanite (Naray-Szabo *et al.*, 1929) contrasts with that of yoderite in intergrowth with kyanite; c is a common direction in both cases, but the common plane is (100) of kyanite in the former and (010) in the latter instance. Fe^{2+} and OH^- ions lie on {010} planes in staurolite, which are parallel to the AlO_6 chains and therefore there is no significant (1 %) increase in chain length. The repeat distance normal to the $Fe(OH)_2$ layers, b_s 16·52 Å., is however of the order of 18 % greater than the corresponding dimension for two units of kyanite structure. The absence of such a strongly directed expansion, the difference in relative orientation, and crystallochemical considerations indicate that yoderite is not analogous to staurolite in its relationship to the kyanite structure.

Subsidiary reflections.

Sharp weak extra reflections occur between the layer lines on heavily exposed b- and c-axis but not on a-axis oscillation photographs. The separation of the subsidiary reflections from the principal layer lines was determined accurately and corresponds to $k = n \pm 0{\cdot}165$, $n \pm 0{\cdot}417$ and $l = n + \frac{1}{2}$; the values of the fractional indices may be expressed approximately, though perhaps without much significance, as $\frac{2}{12}$ (= 0·167) and $\frac{5}{12}$, corresponding to twelvefold multiplication of the b parameter with systematic absence of all but the $12n$ (strong), $12n \pm 2$, $12n \pm 5$ layer lines. Weissenberg photographs of the zero and fourth layers about the a-axis and of the k 1·417 layer about the b-axis were used to determine the positions of the subsidiary reflections in reciprocal space. Two types of reflections occur, type I with indices $n.\ n' \pm 0{\cdot}417.\ n'' \pm \frac{1}{2}$, and type II with indices $n.\ n' \pm 0{\cdot}167.\ n''$. The diffraction pattern of yoderite is thus characterized by pairs of subsidiary reflections sym-

metrically separated by a translation corresponding to 0·083 b^* from absent reflections which would represent halving of b^* and c^*, and by pairs of subsidiary reflections disposed in an identical manner about the strongest principal reflections; the resemblance of this pattern to that exhibited by intermediate plagioclases and investigated in detail by Cole, Sörum, and Taylor (1951), and Gay (1956), is marked. Any dependence of the separation of the subsidiary reflections on composition cannot be investigated at present as all specimens of yoderite from Mautia Hill produce identical diffraction patterns. Any convincing attempt at explanation of the subsidiary reflections is difficult in a mineral whose structure is undetermined and in which possibilities of the occurrence of ordered sequences in the distributions of Al and Si, Mg and Al, OH and O occur. The very small atomic scattering factor of H, however, makes it unlikely that ordering of the OH distribution could give rise to the observed effects.

The assignment of Al atoms exclusively to sixfold positions and Si atoms to fourfold positions in kyanite provides a completely ordered structure in which no extensive substitution by other cations is known to occur, and it is not surprising to find a complete absence of subsidiary reflections on heavily overexposed c-axis oscillation photographs of kyanite. In staurolite Fe^{2+} and OH^- ions separate blocks of kyanite structure to produce a completely ordered structure, and subsidiary reflections failed to appear on a c-axis oscillation photograph heavily overexposed to Fe-$K\alpha$ radiation. Subsidiary reflections are lacking too on c-axis oscillation photographs of lusakite, which has a structure analogous to staurolite (Skerl and Bannister, 1934). Agrell and Smith (1957) have observed in mullite diffraction patterns certain weak non-integral reflections, which are similar to those of the intermediate plagioclases; such subsidiary reflections may be tentatively related to either the presence of Si and Al in ordered sequences in fourfold positions, or to some degree of ordering in the distribution of 39 O^{2-} between forty available positions, or both.

If the analogy between the inferred structure of yoderite and that of kyanite is as good as has been suggested, the possibility of the subsidiary reflections being due to Si–Al ordering may be ruled out because subsidiary reflections are not observed and such ordering cannot occur in kyanite; thus the subsidiary reflections observed in yoderite may be regarded as related to the presence of ordered sequences in the distribution of Mg and Al in equivalent or nearly equivalent positions.

Heat treatment. Single crystals were subjected to successive heatings so that each crystal had an effectively isothermal history. Temperatures were controlled by a platinum resistance thermometer and continuously recorded by a chromel-alumel thermocouple; a constancy of $\pm 5°$ C. was maintained between successive heatings. Quenching by cooling in air to room temperature took < 3 minutes. After each heating the crystals were examined by oscillation photographs (15° oscillation) about the *b*-axis with the X-ray beam, accurately set by Laue photograph, in a standard orientation $\perp(403)$; this orientation causes the reciprocal lattice point corresponding to one of the strongest of the subsidiary reflections $1.1{\cdot}417.\bar{\frac{1}{2}}$ to be intersected by the sphere of reflection near the middle of the oscillation. The intensities of this reflection and of two principal reflections (assumed to be unaffected by heating) were measured by visual comparison with a linear intensity scale and the intensity I of reflection $1.1{\cdot}417.\bar{\frac{1}{2}}$ after heating at $T°$ C. for t hours was expressed as a fraction of its initial intensity I_0. As a check on the generality of the intensity variation of $1.1{\cdot}417.\bar{\frac{1}{2}}$, measurements were made of the intensity of the other strong subsidiary reflection $0.1{\cdot}417.\frac{1}{2}$ for heatings at 730° C., and a similar variation was found. No study has been made of the behaviour of type II reflections.

The experimental data can be fitted empirically to a rate law of the form $i-1 = kt$, where $i = \sqrt{I_0/I}$ and k is a constant. Such a law cannot be rationalized until a structure determination and an interpretation of the subsidiary reflections become available; however, if the process by which the subsidiary reflections decrease in intensity is one of disordering, and if the degree of long-range order α is given by an expression of the form $I/I_0 = (1-\alpha)^2$, as it is in the rather simpler case of order–disorder transitions in cubic alloys (Wilchinsky, 1944), then the rate law would represent second order kinetics for a disordering process. At 795° C. the data clearly fit the second order better than the first order law $\log i = kt$, but at other temperatures either law will fit the experimental data within the rather large limits of error imposed by the inaccuracy of intensity measurement. The nature of the problem precludes the application of more sensitive kinetic criteria for the order of reaction. Since there is no reason to suppose that any change of mechanism occurs with variation in temperature a second order law will be assumed to apply to the process (fig. 2 (i)). At temperatures investigated in the range 700° C. to 817° C. the subsidiary reflections decrease in intensity and vanish if the heating is sufficiently prolonged; they maintain their position, sharpness, and shape unchanged. Below 700° C. the rate of change of intensity was

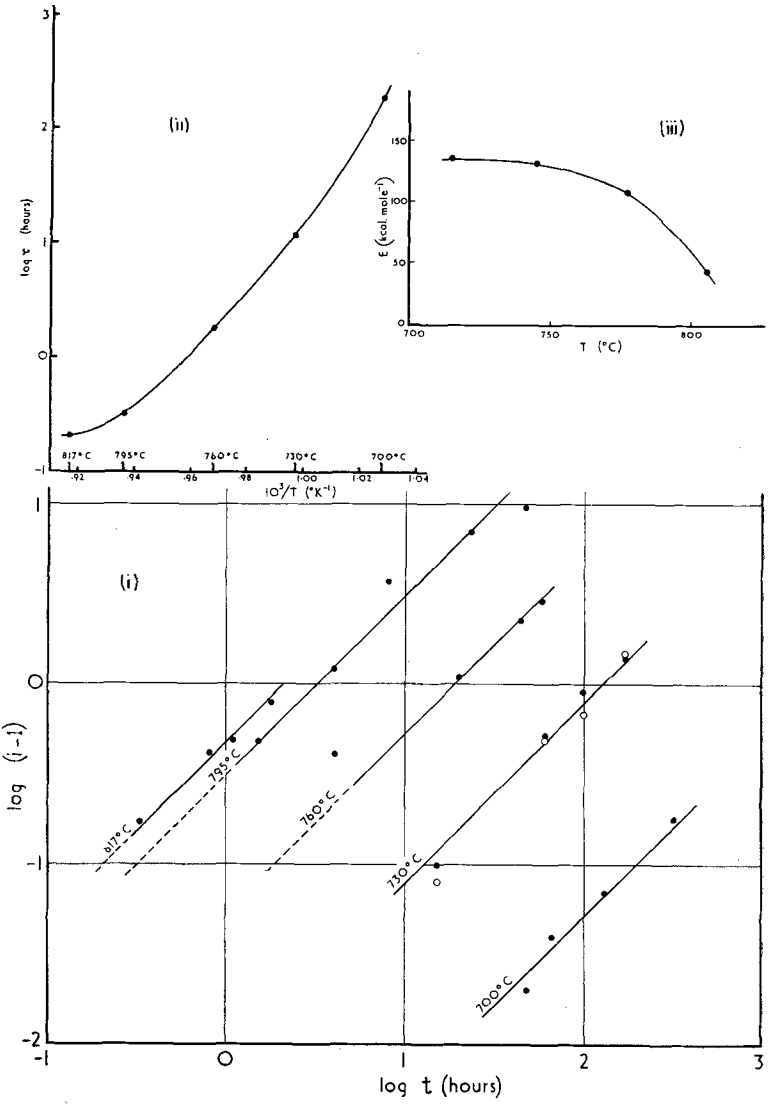

FIG. 2. (i) Plot of $i-1 = kt$; • refers to $1.1 \cdot 417.\frac{1}{2}$, ◦ refers to $0.1 \cdot 417.\frac{1}{2}$. (ii) Plot of $\log \tau = E/RT + B$. (iii) Plot of activation energy against temperature.

too slow for convenient observation, and at 850° C. slow decomposition of the yoderite structure had begun.

It is convenient to designate the state of yoderite without subsidiary reflections, which is stable above some critical temperature less than 700° C., as high-yoderite, and to refer to yoderite with subsidiary reflections as low-yoderite. All kinetic observations have thus been made in the region in which low yoderite is metastable, and the rate of the transformation process at 700° C. is so sluggish that it would seem that transitional thermal states corresponding to subsidiary reflections of diminished intensity are inaccessible to kinetic observation, in contrast to order–disorder transitions in certain alloys, where transitional states of partial ordering rapidly approach equilibrium. That the kinetic observations have been made for transition from a metastable to a stable state does not invalidate the conclusions drawn from those data in the next paragraph, but does preclude any inferences about the thermodynamic equilibrium between the high and low thermal states.

In considering the temperature coefficient of the rate of reaction it is convenient to assume a relationship of the form $\tau = Ae^{E/RT}$, where τ is the time required for a given fraction of the transformation to take place isothermally at $T°$ K., i.e. the time corresponding to a given value of i, and A is a constant.[1] A plot of this expression in the form $\log \tau = B + E/RT$ is shown in fig. 2 (ii). If the observed process is an order–disorder transition, E may be taken to represent the energy barrier which an ion must surmount to pass from a position of order to become part of a disordered array. The value of E will be expected (Bragg, Sykes, and Bradley, 1937) to decrease as T rises, since each ion will then have more of its neighbours in the disordered state; such a decrease is observed (fig. 2 (iii)) from values in the region of 140 kcal. per gram-ion at 700° C. to 40 kcal. per gram-ion at 817° C.

Values of the activation energy E of the process will be independent of the correctness of any order–disorder interpretation of I/I_0 and of the right choice of rate law. Such activation energies, for which no more than approximate accuracy is claimed, should correspond to those characteristic of the diffusion of cations through a silicate lattice, since in each case momentary displacement of ions from lattice positions must occur. No comparable data are available for the diffusion of cations

[1] This expression is a form of the Arrhenius equation $k = Ae^{-E/RT}$ familiar in gas and solution kinetics, where it has a theoretical basis. It can readily be seen that $k\tau$ = constant. By considering τ instead of k, uncertainty about the precise significance of i is eliminated.

through silicate lattices, but in metals a large collection of data covers the range 10 to 100 kcal. per gram-atom and in salts, other than those of abnormally high conductivity, conductivity measurements lead to values of the activation energy for diffusion from 10 to 50 kcal. per gram-ion (Barrer, 1951, p. 275).

The effect of a non-oxidizing atmosphere, that is nitrogen with a low oxygen content corresponding to $p_{O_2} \sim 10^{-20}$ atm. (i.e. in the presence of metallic iron at the same temperature as the specimen), on the rate of decrease of intensity of $1.1{\cdot}417.\bar{\frac{1}{2}}$ was found to be negligible within the limits of experimental error in one heating at 760° C. at 1 atm. total pressure.

Discussion. The subsidiary reflections in yoderite are sharp, consistent in position and intensity with the monoclinic symmetry of the pseudo-lattice, and have constant separation in the b^* direction of reciprocal space from principal reflections (type II) or from absent reflections (type I), such parent reflections corresponding to an A-centred lattice of dimensions a, $2b$, $2c$, β; they remain unchanged in position and their sharpness persists until they vanish on heating. Neither type appears to exhibit any systematic absences. Members of each pair of type I reflections, $h.(2k+1)/2 \pm 0{\cdot}083.l+\frac{1}{2}$, commonly differ in intensity, and even on heavily exposed photographs in some cases only one member of a pair may be detectable. Asymmetry is likewise observed in the intensity of pairs of type II reflections, $h.k \pm 0{\cdot}167.l$, except for k zero. No regularity is discernible in the occurrence of one or both members of split reflection pairs, nor in the variation of intensity with h, k, or l. Type II reflections are always associated with principal reflections of higher intensity, the strongest principal reflections tending in general to have relatively strong satellites; reflections $h.0 \pm 0{\cdot}167.l$ may be of non-zero intensity and are then symmetrical as required by the monoclinic symmetry. The form of the variation of intensity of type I reflections with temperature has been indicated in the preceding section.

The properties of type I reflections are very like those of normal type (*b*) subsidiary reflections in the intermediate plagioclases, especially in the more An-rich part of the series (Gay, 1956), except that on heating in the range 950° C. to 1200° C. the latter become diffuse before they finally disappear (Gay and Bown, 1956). Type II reflections correspond likewise to satellites well known in the intermediate plagioclases (Bown and Gay, 1958). The subsidiary reflections in mullite (Agrell and Smith, 1957) are split in directions other than that of the AlO_6 octahedral chains and consequently differ from those in yoderite in their orientation

relative to the presumed common elements of the mullite and yoderite structures. No adequate explanation of the plagioclase and mullite phenomena has yet been given.

Lipson (1950) has reviewed the several types of superlattice produced by ordering in alloys and their diffraction effects; none gives rise to subsidiary reflections analogous to those of yoderite.

Chayes (1958) has discussed the subsidiary reflections of intermediate plagioclase in terms of a simple statistical model of short-range disorder, without attempting to explain how the observed diffraction pattern is produced. In explaining the diffraction effects characteristic of the intermediate plagioclases and yoderite the essential problem is, however, not one of statistics but of diffraction theory. Megaw (1957) has approached this aspect of the problem with a model involving the presence of stacking faults; while the diffraction theory of such a structure has not yet been fully explored, some measure of explanation has been achieved.

An analogy may be drawn between the subsidiary reflections in yoderite and the effects produced by two common types of ruling error in optical diffraction gratings. A periodic error in spacing gives rise to Rowland ghosts, which are subsidiary spectra situated symmetrically close to principal spectra; they correspond to the subsidiary reflections due to periodic variation of lattice spacing observed for instance in Cu_4FeNi_3. Lyman ghosts lie far from the parent line, being nth harmonics of a fundamental period of error N, where N is large and n/N is close to some simple fraction; they occur in small groups n, $n+1$, $n+2$, &c., and are very weak. The appearance of Lyman ghosts is due to an error involving two periods that are incommensurate with each other (Meyer, 1934) or a single error of very short period. The attribution of type I subsidiary reflections in yoderite to such a variation in atomic scattering factor, perhaps combined with a like variation in lattice parameter, would seem reasonable, although simple calculation fails to produce significant results for the periods of variation.

The solution of the problem of the subsidiary reflections in yoderite must await a complete structure determination. It would appear, however, that since the reflections are split in the direction of the dyad axis the problem represents a simplification of that of the intermediate plagioclases.

Thermal decomposition.

Powder data. Finely ground specimens of yoderite were heated in unsealed platinum envelopes in alumina crucibles at various tempera-

tures. After being held at the requisite temperature for a convenient time, the specimen was allowed to cool in air to room temperature and then examined on the X-ray diffractometer with Cu-$K\alpha$ radiation. A series of traces for the range 2θ 20° to 40° is shown in fig. 3.

After 72 hours at 950° C. the yoderite pattern, fig. 3 (i), has completely disappeared and given way to mullite and an unidentified phase, fig. 3 (ii), the very strong mullite peak at 2θ 26·2° being present as a weakened broadened peak, which may also involve the second phase; oxidation has occurred and the mauve colour of yoderite powder has become dull yellow. The formation of mullite at this temperature is not indicated by the phase diagram and must be regarded as a kinetically controlled reaction leading to a metastable product; the structure of yoderite becomes unstable at 840° C. ($\pm$20°) (inferred from single crystal data) and portions of the structure undergo slight rearrangement to form metastable mullite, a process involving a lower activation energy than the formation of the assemblage, 68 % cordierite+32 % sapphirine, that would be thermodynamically stable but which, inheriting no structural elements from yoderite, would require a higher activation energy for its formation. After a further 75 hours at 1100° C. the pattern has again altered fundamentally; indialite and sapphirine are accompanied by a small amount of mullite. Single crystal data indicate that the formation of indialite begins at 1040° C. The indialite peaks are displaced slightly to the high θ side of those, fig. 3 (vi), of indialite (Miyashiro *et al.*, 1955). That indialite rather than cordierite is present is shown by the shape of the critical peak at 2θ 29½°; the metastable formation of indialite is usual at temperatures greater than 830° C. At 1180° C. (70 hours) the same pattern was observed, with increase in the strength of the sapphirine peaks relative to indialite, At 1270° C. (120 hours), fig. 3 (iii), and 1345° C. (90 hours) indialite and sapphirine are present and evidence of a small content of mullite persists. The relative strength of the sapphirine peaks increases steadily, producing a step on the high θ side of the 2θ 29½° indialite peak. The colour of the powder gradually changed from dull yellow at 950° C. to medium brown at 1345° C., where considerable contraction occurred to produce a hard cake; incongruent melting may be presumed to begin between 1270° C. and 1345° C. After a further 12 hours at 1415° C., fig. 3 (iv), the indialite pattern disappears; sapphirine and mullite are present and the specimen is in the form of a hard green cake.

Single crystal data. In heating experiments below 850° C. no change was discernible in the quality of the principal reflections. Incipient

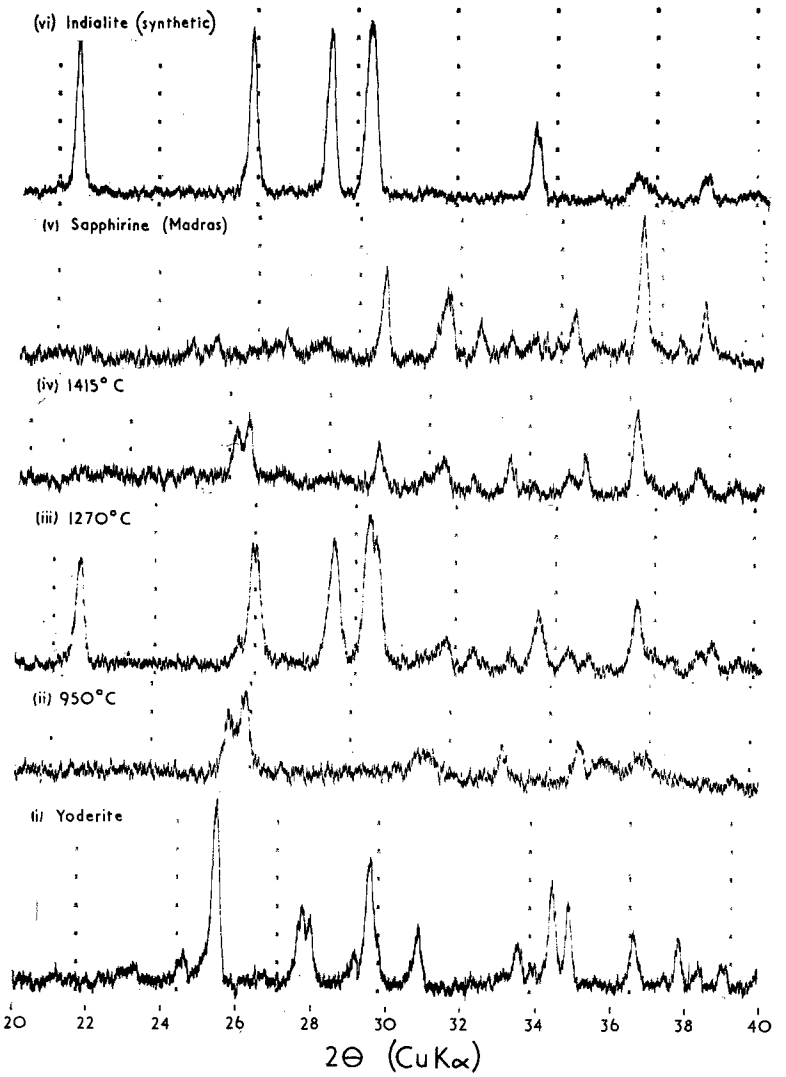

FIG. 3. Diffractometer traces of yoderite and the products of its thermal decomposition.

thermal decomposition of yoderite, indicated by the increased size of Laue reflections, was observed in a crystal heated for about 150 hours at 850° C.; similar effects were observed after about 80 hours at 900° C. At 1000° C., however, decomposition has become much more rapid, and after 1 hour no yoderite reflections persist on *b*-axis oscillation photographs. Partial decomposition to mullite was observed in a crystal heated for 10 minutes at 1000° C. and the relative orientation of the mullite and yoderite lattices was obtained from zero, first, and second layer Weissenberg photographs about the *b*-axis of yoderite. The AlO_6 chain direction, *b* in yoderite and *a* in mullite, is common and the *a*-axis of mullite is 4° (±2°) from the *c*-axis of yoderite; in part at least the AlO_6 chains would thus appear to remain nearly constant in orientation, while cross-linkages are rearranged and part of the unit-cell contents of yoderite diffuse out of the domains of the new mullite lattice. Mullite reflections are streaked along θ curves and their relatively high intensity centres occupy a large volume in reciprocal space, consistent with the expected small size and departure from perfect orientation of the units of mullite structure. The Weissenberg photographs also exhibit reflections that can be indexed on an orthorhombic lattice of dimensions *a* 5·78 Å., *c* 5·72 Å. (±0·05 Å.), with $a||b$ of yoderite and $b||a$ of yoderite, not corresponding to any known phase in the MgO–Al_2O_3–SiO_2–H_2O system.

At 1040° C. powder lines of indialite showing no preferred orientation appear. The rate of formation of units of indialite structure large enough to give sharp powder lines appears to be rapid, in that 20 minutes at 1045° C. are adequate to produce a sharp pattern, whereas 1 hour at 1035° C. produces no indialite pattern at all. The process is envisaged as the formation of nuclei of indialite among the disorganized array of cations distributed through the oxygen lattice outside the mullite crystallites; at temperatures above the critical temperature for nucleation of indialite, 1040° C., grain growth is so rapid that no intermediate stages with broadened powder rings are observed. Single crystal reflections of mullite and of the orthorhombic phase persist for at least 17 hours at 1100° C. and were observed on a zero layer Weissenberg photograph about the *c*-axis of mullite; the reflections are more markedly streaked along θ curves than at lower temperatures.

The formation of mullite is accompanied by the oxidation of Fe^{2+} ions, indicated by the development of a dull yellow colour in the crystal; Fe^{3+} can substitute readily for Al^{3+} in the mullite lattice. Heating at atmospheric pressure in N_2 with a low oxygen content corresponding to the

iron–iron-oxide equilibrium ($p_{O_2} \sim 10^{-15}$ atm.) facilitates the thermal decomposition of yoderite. Mullite and indialite are present and yoderite persists after 21 hours at 900° C.; yoderite, however, is completely decomposed to mullite and indialite in 1 hour at 1000° C. In both experiments the crystal became dull grey in colour. It is inferred that reduction of Fe^{3+} takes place simultaneously with dehydration, a process which involves the thorough disruption of the yoderite structure to produce an environment more favourable for the nucleation of indialite than that provided by the material expelled from the relatively large units of mullite structure under oxidizing conditions, where an approximately close-packed oxygen lattice may persist and give rise to a high energy of nucleation of indialite; at low p_{O_2}, however, the critical temperature for indialite nucleation is lowered by $> 140°$ C. and mullite crystallites are smaller and less well oriented.

Differential thermal analysis and thermogravimetric analysis. Differential thermal analyses in oxygen and in nitrogen at atmospheric pressure have very kindly been made for me by Dr. R. C. Mackenzie.[1] The run in oxygen was made on 30 mg. yoderite mixed with 10 mg. calcined kaolinite sandwich-packed in a nickel holder, and exhibited significant endothermic peaks at 500° C. and 917° C.; a strong exothermic peak begins above 950° C. at the end of the trace. The run in nitrogen was made on 47 mg. yoderite mixed with 10 mg. calcined kaolinite sandwich-packed with 140 mg. calcined kaolinite in a ceramic holder, and exhibited significant endothermic peaks at 486° C. and 888° C. and a strong exothermic peak beginning above 900° C. near the end of the trace. There is thus no marked difference between the runs and it is inferred that oxidation of Fe^{2+} is one of the reactions represented by the exothermic peak above 900° C., which is incompletely displayed on the traces.

In an attempt to elucidate the endothermic peak at 486–500° C. a thermogravimetric analysis was very kindly made for me by Dr. J. R. Butler[2] on an 884·7-mg. sample of yoderite. No significant weight loss ($< 0{\cdot}1$ %) occurred between 20° C. and 1050° C.; at 1050° C. the sample began to lose weight rapidly and reached a constant weight at 1125° C., where the weight loss amounted to 2·96 %. No further change in weight occurred between 1125° C. and 1200° C., and no increase in weight was observed on cooling overnight to room temperature. If the loss in weight above 1050° C. represents dehydroxylation and oxidation

[1] The Macaulay Institute for Soil Research, Aberdeen.

[2] Department of Geology, Imperial College of Science and Technology, London.

of Fe^{2+}, the analysis of table I indicates that it should amount to 2·65 %; the FeO determination is however subject to some uncertainty and a loss of 2·96 % would correspond to a rather lower FeO content of 2·25 %, or to incomplete oxidation.

Differential thermal, thermogravimetric, and X-ray data indicate that oxidation must accompany dehydroxylation and nucleation of metastable mullite, a complicated process giving rise to the strong exothermic peak above 950° C., correlated with the rapid weight loss beginning at 1050° C. and the appearance of reflections due to mullite on single crystal photographs after brief heating at 1000° C. or after prolonged heating as low as 850° C. The small endothermic peak (at 915° C.) preceding this exothermic change has some counterpart in kaolinite, where the third endothermic peak (Mackenzie *et al.*, 1957, p. 107) immediately precedes the main exothermic peak and may be interpreted in terms of an entropy increase due to a structural rearrangement; alternatively the peak at 915° C. in yoderite may correspond to endothermic dehydroxylation, followed by exothermic nucleation of mullite above 950° C.

For the small endothermic peak at 486–500° C. no explanation can be offered.

The colour of yoderite.

The intense colour of yoderite requires explanation in the absence of a significant content of any simple ionic chromophore such as Cu or Co. The blue colour of minerals containing iron in two valence states is well known and has been reviewed by MacCarthy (1926), Weyl (1951*a*), and others; it appears to be due to the presence of a chromophore group Fe^{3+}–O–Fe^{2+} in which electron exchange $Fe^{2+} \rightleftharpoons Fe^{3+} + e^-$ is facilitated by the high polarizability of O^{2-}. Such exchange is inhibited by anions of low polarizability, and the presence of layers of OH^- or F^- ions in a structure will give a strongly directional character to the absorption, as Weyl (1951*b*) has observed in biotite. Familiar examples of blue ferrous–ferric compounds are Prussian Blue and the alkali amphiboles with a wide range of FeO/Fe_2O_3 values and total iron contents; compounds of very high iron content such as magnetite exhibit very strong absorption and appear black. Yoderite has a high FeO/Fe_2O_3 value of 9·6 and low total iron calculated as FeO 5·27 %. On heating in an oxidizing atmosphere above 950° C. it becomes pale yellow, the colour change moving inwards from the margins of the grain as the time of heating is increased; at 900° C. in nitrogen at low p_{O_2} yoderite becomes greenish grey and it is inferred that reduction has accompanied dehydration.

The blue colour of glasses in which di- and tri-valent iron are in equilibrium has been the subject of a considerable amount of experimental study, summarized by Weyl (1951*a*). Such glasses are characterized by a strong absorption minimum in the region 550–700 mμ, bounded by the Fe^{3+} absorption band in the near ultra-violet and violet end of the visible range and by the 1100 mμ absorption band of Fe^{2+}.

Paragenesis and stability relations.

The chemical analysis of a talc-rich specimen of quartz–yoderite–kyanite–talc schist is shown in table III; the composition of the yoderite-

TABLE III. Chemical composition of quartz–yoderite–kyanite–talc schist and of talc.

	1.		2.		3.	
SiO_2 ...	74·54	SiO_2 ...	63.49	Si^{4+} ...	3·98	
TiO_2 ...	0·27	Al_2O_3 ...	3·95	Al^{3+} ...	0·29	
Al_2O_3 ...	8·13	FeO ...	0·56	Fe^{2+} ...	0·03	
Fe_2O_3 ...	1·92	MnO ...	0·06	Mn^{2+} ...	—	2·85
FeO ...	0·90	MgO ...	26·66	Mg^{2+} ...	2·49	
MnO ...	0·11	CaO ...	0·64	Ca^{2+} ...	0·04	
MgO ...	12·33	H_2O+ ...	4·64	O^{2-} ...	10·00	
CaO ...	trace	H_2O- ...	0·12	OH^- ...	1·94	
Na_2O ...	0·14		100·12			
K_2O ...	0·03					
CO_2 ...	nil					
P_2O_5 ...	trace					
H_2O+ ...	1·59					
H_2O- ...	0·28					
	100·24					

1. Analysis of quartz–yoderite–kyanite–talc schist, Mautia Hill, Tanganyika. JH 2563/2. Analyst: W. H. Herdsman.

2. Analysis of talc, Mautia Hill, Tanganyika. JH 2563/2. Total iron recorded as FeO. Analyst: A. J. Radford.

3. Unit-cell contents of talc, corresponding to 10 O^{2-} per unit cell, calculated from analysis of column 2 omitting H_2O-.

bearing rocks ranges from that of the analysed specimen towards quartz. The analysis essentially represents a high silica composition in the MgO–Al_2O_3–SiO_2–H_2O system (fig. 4) and is characterized by a virtually complete lack of Ca and alkalis, high Mg/Fe, and the presence of 8 % corundum and 31 % enstatite in the norm. Such a composition differs markedly from that of any igneous rock or common sediment; three rather specialized possibilities remain: the rock may result from the metamorphism of a tectonic mixture of quartz with an igneous ultra basic rock, or may be a product of magnesian metasomatism, or of the

isochemical metamorphism of a saponitic bentonite. The first is improbable on the grounds that no source of ultrabasic material is discernible and that it is difficult to reconcile the high alumina content with absence of Ca and Na. The second would require magnesian metasomatism of an

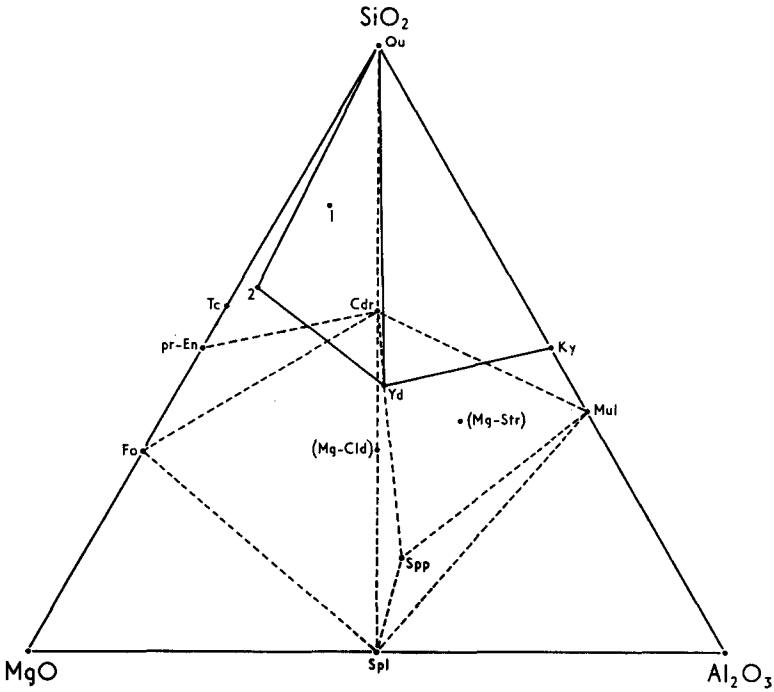

FIG. 4. Projection of the MgO–Al_2O_3–SiO_2–H_2O system from the H_2O apex. Solid lines show phase assemblages at Mautia Hill. Dashed lines show phase assemblages at the solidus in the dry system. Key: 1, quartz–yoderite–kyanite–talc schist; 2, talc from 1; Cdr, cordierite; Fo, forsterite; Ky, kyanite; (Mg-Cld), hypothetical magnesian chloritoid; (Mg–Str), hypothetical magnesian staurolite; Mul, mullite; pr-En, proto-enstatite; Qu, quartz; Spl, spinel; Spp, sapphirine; Tc, talc; Yd, yoderite.

argillaceous sandstone, the introduction of Mg being associated, as is usual (Eskola, 1914), with loss, in this case complete, of Ca and alkalis. The occurrence of an argillaceous sandstone interstratified with a manganiferous sandstone and a limestone is stratigraphically consistent; that Mg should have been fixed in this semi-pelite but not in the adjacent piemontite–quartzite might well have been controlled, or at least facilitated, by the prior existence of a high content of phyllosilicate

minerals, at once providing a local concentration of slip-planes during tectonic movement, and therefore channels for the admission of Mg-bearing solutions, and on a molecular scale a structural framework sufficiently similar to that of talc for the replacement of Ca and alkalis by Mg to occur under conditions favouring the nucleation of talc, excess Al being segregated in kyanite or some other aluminous mineral that became kyanite during subsequent metamorphism. The source of the Mg would appear to have been entirely external and unrelated to the dolomite-free character of the adjacent crystalline limestone, which therein differs from most Archaean limestones in Tanganyika. The third possibility perhaps provides the fewest difficulties; the present composition of the rock lies at low temperatures in the field of synthetic montmorillonite–quartz–talc (Roy and Roy, 1955) and is approximately analogous to natural chert-bearing saponitic bentonites, which may be produced under a variety of conditions from basic pyroclastics by weathering *in situ* (Ross and Hendricks, 1945, p. 64), the peculiarity of this occurrence being the very low calcium content. The work of Roy and Roy (1955) has shown that montmorillonite decomposes at temperatures less than 500° C. to give rise at this composition to a quartz–talc–pyrophyllite assemblage stable up to 530° C. at p_{H_2O} 667 bars, where cordierite formation begins, accompanied at 575° C. by the decomposition of pyrophyllite to cristobalite and mullite. If these two latter reactions are inhibited, as would seem probable, by increased pressure, and pyrophyllite decomposes, without the prior formation of cordierite, to silica and kyanite, the assemblage that apparently existed before the formation of yoderite will have been developed.

The yoderite-bearing rocks are composed principally of talc and quartz with some 10 % of yoderite-rimmed kyanite and accessory hematite. The chemical analysis of talc from the analysed rock is set down in table III; with an alumina content of 3·95 %, corresponding to 15 % of the pyrophyllite molecule in solid-solution, it is one of the most aluminous natural occurrences of talc known and reflects the relatively aluminous nature of the environment. Yoder (1952) has observed that synthetic talc growing in aluminous media can apparently take a considerable amount of pyrophyllite into solid solution. The talc is pale flesh-pink in hand-specimen and has $2V_{\alpha}$ 6°, β 1·592 ($\pm$0·002). The kyanite is remarkable for its light brown colour in hand-specimen, contrasting with the grass-green colour of kyanite in the kyanite–biotite gneiss at Mautia Hill. The brown kyanite contains[1] a marked content of

[1] Qualitative spectrographic analysis by Dr. S. R. Nockolds.

Mn, a small content of Fe, about 100 p.p.m. Cr, about 100 p.p.m. Zr, a trace of Ti, and about 20 p.p.m. Ga, with Ni, Co, V, Na below the limits of sensitivity. The green kyanite contains rather less Mn, Fe, Ti, about 50 p.p.m. Cr, and about 20 p.p.m. Ga, with Zr, Ni, Co, V, Na below the limits of sensitivity. The colour of the brown kyanite may be tentatively attributed to the presence of Mn^{3+}, while the green colour may be due to Fe in the presence of a rather lower Mn content. The identification of hematite was confirmed by its X-ray powder pattern.

Whatever may have been the early history of the rock, the assemblage talc–kyanite–quartz was eventually generated, presumably in the presence of excess water vapour. However, according to Yoder's (1952) experimental work, talc and kyanite can have no stable coexistence at pressures below 1000 bars. Kyanite may perhaps have formed metastably at low temperatures in the presence of talc, perhaps in the manner suggested in a previous paragraph. When the temperature subsequently increased, talc and kyanite reacted to produce, not cordierite and water vapour as might be expected, but the hydrous mineral yoderite. In seeking an explanation of this it may be instructive to consider the volume change for the relevant reactions:

(i)	Tc	+	3 Ky	+	0·5 Qu	⇌	1·5 Cdr	+	H_2O		
	140 c.c.		135 c.c.		11 c.c.		337 c.c.		34 c.c.	$\Delta V = +85$ c.c.	
(ii)	Tc	+	3 Ky	+	0·3 H_2O	⇌	1·1 Yd	+	2.5 Qu		
	140 c.c.		135 c.c.		10 c.c.		216 c.c.		65 c.c.	$\Delta V = -13$ c.c.	

The gram-formula volume indicated beneath each solid phase will be independent to a first approximation of pressure and temperature. The conditions represented are T 500° C., p_{H_2O} 1000 bars, the corresponding density of water, 0·532 g./c.c., being taken from Kennedy (1950); under these conditions equation (i) represents the formation of cordierite with a volume increase of 30 %, and equation (ii) the formation of yoderite with a volume decrease of 5 %. The magnitude of these volume changes will decrease with declining temperature and increasing pressure, but ΔV for equation (i) will remain positive and for equation (ii) negative at all temperatures and pressures; thus throughout the petrogenetically interesting PT range the formation of cordierite by equation (i) will be inhibited and that of yoderite by equation (ii) facilitated by high pressure. An upper limit to the temperature at which yoderite can form is set by the univariant curve of talc decomposition (Bowen and Tuttle, 1949) reproduced in fig. 5. At p_{H_2O} 1000 bars talc is stable below 795° C. and at least as low as 400° C. Temperatures in excess of 850° C.

cannot therefore have prevailed at Mautia Hill and would not in any case be expected. A minimum pressure limit is set by the univariant curve of the kyanite–sillimanite transition (Clark, Robertson, and Birch, 1957), also shown in fig. 5. It should be noted that the attainment of equilibrium at the Al_2SiO_5 composition even in the presence of significant p_{H_2O} is remarkably sluggish; however, at high temperatures kyanite inverts rapidly to sillimanite and therefore the region below the

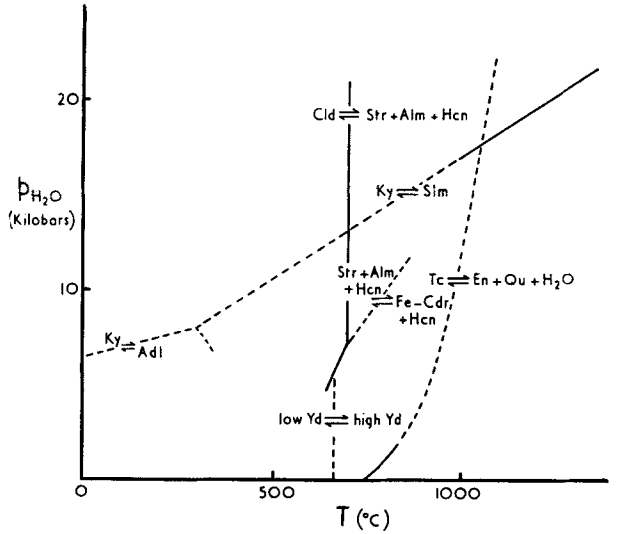

FIG. 5. p_{H_2O}–T diagram illustrating the stability relations of yoderite. Key: Adl, andalusite; Alm, almandine; Cld, chloritoid; En, enstatite; Fe-Cdr, iron-cordierite; Hcn, hercynite; Ky, kyanite; Qu, quartz; Slm, sillimanite; Str, staurolite; Tc, talc; Yd, yoderite.

kyanite curve beyond about 500° C. may be regarded as outside the likely *PT* conditions at Mautia Hill during the formation of the talc–quartz–kyanite assemblage.

The existence of subsidiary reflections in yoderite indicates that the yoderite-bearing rocks must have cooled slowly through the range immediately below the lower limit of stability of high-yoderite, as the rate of the transition process must soon become prohibitively slow as temperature falls. Alternatively the transition from high-yoderite to low-yoderite may well have no significant rate under any conditions and low-yoderite may be able to form only during crystallization. The low→high transition temperature in yoderite appears to be just below

700° C. at 1 atm., and no data are yet available on its pressure coefficient; crystallization of yoderite in the range immediately below 700° C. would not be inconsistent with any of the factors discussed in the previous paragraph. Gay and Bown (1956) have considered the analogous problem of thermometric inferences from the structural state of intermediate plagioclase, where transitional states are also observed.

That the formation of yoderite will be favoured by high p_{H_2O} can be seen from fig. 4. At low p_{H_2O} the assemblages talc–cordierite–quartz and kyanite–cordierite–quartz are stable. At higher total pressure and presumably at high values of p_{H_2O} the assemblages talc–yoderite–quartz–water and kyanite–yoderite–quartz–water become stable. Assemblages containing yoderite and cordierite have not been observed at Mautia Hill; they would be presumed to correspond to relatively low values of p_{H_2O}. Yoder (1952) studied the cordierite composition at various temperatures and p_{H_2O} 1000 bars, and Roy and Roy (1955) studied the composition $23MgO:28Al_2O_3:49SiO_2$ at 515° C. and p_{H_2O} 667 bars; neither studied any composition nearer that of yoderite, $27MgO:29Al_2O_3:44SiO_2$ and therefore it cannot be inferred that the lower stability limit of yoderite is as high as 667 bars.

Recent experimental work on the stability relations of staurolite (Halferdahl, 1957) may throw some light on the stability field of yoderite; although their structures are distinct, both minerals may be regarded as hydrous modifications of the kyanite structure. Staurolite is stable at all $p_{H_2O} > 7000$ bars and temperatures greater than about 700° C., below which chloritoid is a stable phase, and lower than a largely undetermined univariant curve which represents the decomposition of staurolite into anhydrous phases. Moreover an upper p_{H_2O} limit emerges for the stable existence of iron-cordierite, represented by the equilibrium Fe-cordierite + hercynite + $H_2O \rightleftharpoons$ staurolite + almandine. Halferdahl's curves, shown in fig. 5, apply only to the iron-chloritoid composition and may be expected to be modified in position, if not in general form, towards the composition corresponding to the iron analogue of yoderite. Structural differences between yoderite and staurolite, and the non-existence of the magnesian chloritoid end-member will further modify the position of the yoderite field in relation to that of staurolite; that yoderite is stable only at p_{H_2O} in excess of about 10 000 bars, and has a lower temperature limit of stability certainly less than 1000° C. and perhaps no greater than 500° C., would be consistent with what evidence there is.

It is difficult to comment adequately on the p_{O_2} conditions under

which yoderite crystallized at Mautia Hill. Hematite inclusions occur in yoderite, which contains iron dominantly in the ferrous state, with $Fe^{3+}/Fe^{2+} = 0{\cdot}09$. Preliminary experimental work suggests that completely ferrous minerals are not stable at higher partial pressures of oxygen than are represented by the equilibrium $2Fe_3O_4 + \frac{1}{2}O_2 \leftrightharpoons 3Fe_2O_3$ at any temperature and any total pressure (Eugster, 1956; Halferdahl, 1957). Its Fe^{3+} content, though small, may enable yoderite to extend into the hematite field, so that over a small range of p_{O_2} at any temperature yoderite and hematite may be in equilibrium in accordance with the petrographic observation at Mautia Hill.

In conclusion it should be stressed that this discussion of the paragenesis of yoderite is speculative. The final elucidation of the metamorphic history of the yoderite-bearing rocks at Mautia Hill must await more detailed study of the petrology of the associated rocks, search for and study of other yoderite occurrences, and an experimental study of the stability relations of yoderite.

Acknowledgements. My thanks are due to Professor C. E. Tilley, F.R.S., for constant advice and encouragement during this work and to Dr. S. O. Agrell, Dr. P. Gay, Dr. J. D. C. McConnell, and Dr. S. R. Nockolds for advice and many helpful discussions. I am indebted to Dr. J. R. Butler for the thermogravimetric analysis, to Dr. R. C. Mackenzie for differential thermal analyses, to Dr. S. R. Nockolds for spectrographic determinations, to Dr. S. O. Agrell for making available to me before publication the text of a further communication by himself and Dr. J. V. Smith on mullite, to Mr. J. H. Scoon for the ferrous oxide determination, and to Mr. K. O. Rickson for taking some of the X-ray photographs. I acknowledge the grant of a Research Studentship by the Department of Scientific and Industrial Research.

References.

AGRELL (S. O.) and SMITH (J. V.), 1957. Abstracts Fourth Internat. Congr. of Cryst., Montreal, p. 32.

BARRER (R. M.), 1951. Diffusion in and through solids. Cambridge University Press.

BOWEN (N. L.) and TUTTLE (O. F.), 1949. Bull. Geol. Soc. Amer., vol. 60, p. 439.

BOWN (M. G.) and GAY (P.), 1958. Zeits. Krist., vol. 111, p. 1.

BRAGG (W. L.), SYKES (C.), and BRADLEY (A. J.), 1937. Proc. Phys. Soc., vol. 49, extra part, p. 96.

CHAYES (F.), 1958. Acta Cryst., vol. 11, p. 323.

CLARK (S. P.), ROBERTSON (E. C.), and BIRCH (F.), 1957. Amer. Journ. Sci., vol. 255, p. 628.

COLE (W. F.), SÖRUM (H.), and TAYLOR (W. H.), 1951. Acta Cryst., vol. 4, p. 20.

ESKOLA (P.), 1914. Bull. Comm. Géol. Finlande, no. 40.

EUGSTER (H. P.), 1956. Ann. Rept. Geophys. Lab. 1955–6, p. 158.

GAY (P.), 1956. Min. Mag., vol. 31, p. 21.

—— and BOWN (M. G.), 1956. Ibid., vol. 31, p. 306.

GROVES (A. W.), 1951. Silicate Analysis, 2nd edn, London.
HALFERDAHL (L. B.), 1957. Ann. Rept. Geophys. Lab. 1956–7, p. 225.
HEY (M. H.), 1941. Min. Mag., vol. 26, p. 116.
KENNEDY (G. C.), 1950. Amer. Journ. Sci., vol. 248, p. 540.
LIPSON (H.), 1950. Progress in Metal Physics, vol. 2, p. 1.
MACCARTHY (G. R.), 1926. Amer. Journ. Sci., ser. 5, vol. 12, p. 17.
MACKENZIE (R. C.) *et al.*, 1957. The Differential Thermal Investigation of Clays. Mineralogical Society, London.
MEGAW (H. D.), 1957. *In* Conference Report, Brit. Journ. Appl. Physics, vol. 8, p. 427.
MEYER (C. F.), 1934. The diffraction of light, X-rays, and material particles. University of Chicago Press.
MIYASHIRO (A.), IIYAMA (T.), YAMASAKI (M.), and MIYASHIRO (T.), 1955. Amer. Journ. Sci., vol. 253, p. 185.
NARAY-SZABO (St.), TAYLOR (W. H.), and JACKSON (W. W.), 1929. Zeits. Krist., vol. 71, p. 117.
ROSS (C. S.) and HENDRICKS (S. B.), 1945. U.S. Geol. Surv., Prof. Paper 205-B.
ROY (D. M.) and ROY (R.), 1955. Amer. Min., vol. 40, p. 147.
SKERL (A. C.) and BANNISTER (F. A.), 1934. Min. Mag., vol. 23, p. 598.
TEMPERLEY (B. N.), 1938. Geol. Surv. Tanganyika, Short Paper 19.
WEYL (W. A.), 1951*a*. Coloured Glasses. Soc. of Glass Technology, Sheffield.
—— 1951*b*. Journ. Phys. Chem., vol. 55, p. 507.
WILCHINSKY (Z. W.), 1944. Journ. Appl. Phys., vol. 15, p. 806.
YODER (H. S.), 1952. Amer. Journ. Sci., Bowen vol., p. 569.

EXPLANATION OF PLATE XI.

FIG. 1. General aspect of quartz–yoderite–kyanite–talc schist. JH 2563/2. Ordinary light, ×4.

FIG. 2. Replacement of talc along cleavage planes by yoderite. JH 2563/2. Plane polarized light, ×110.

FIG. 3. Kyanite relicts in parallel orientation in a grain of yoderite. JH 2563/14. Plane polarized light, ×16.

FIG. 4. The development of yoderite rims to kyanite grains. JH 2563/2. Plane polarized light, ×14.

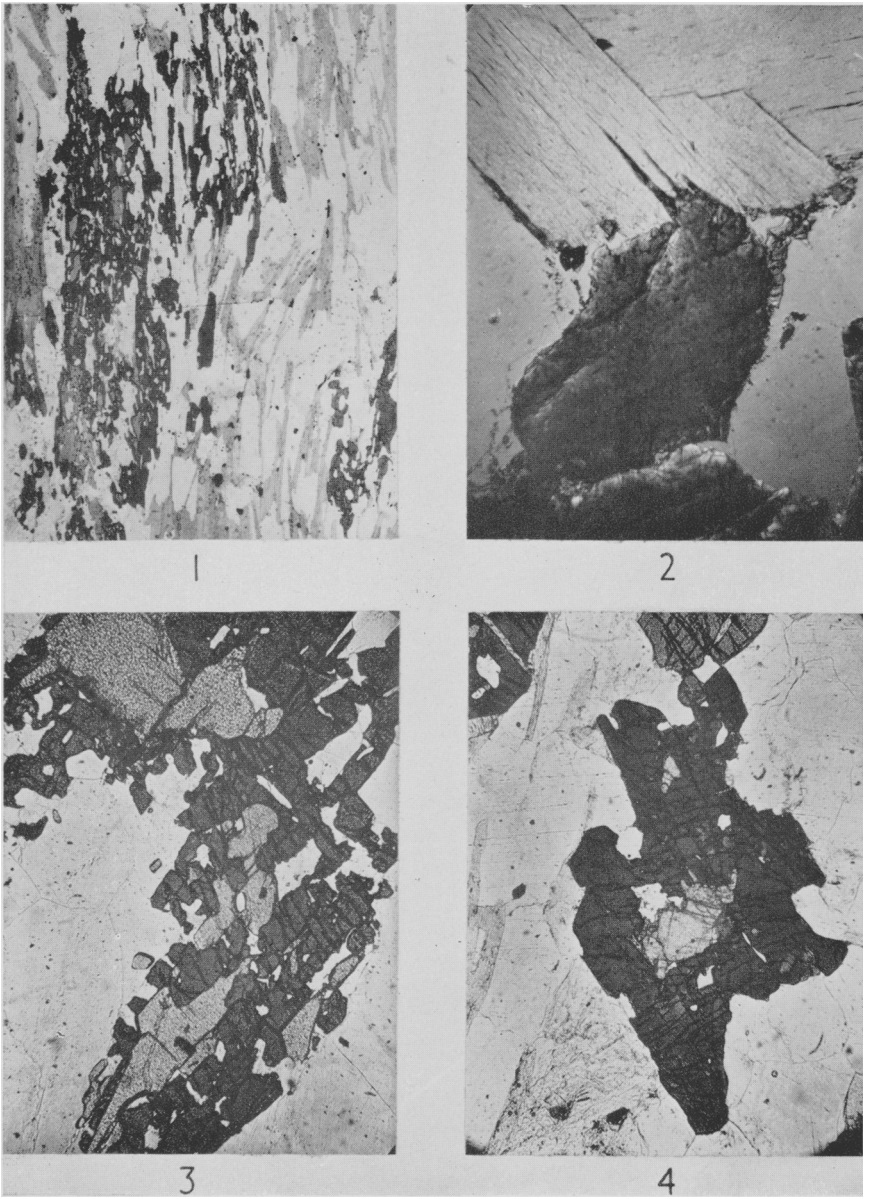

DUNCAN MCKIE: YODERITE